Crystallographic and Molecular Modeling Studies on 3-Ethyl-3-(4-pyridyl)piperidine-2,6-dione and Its Butyl Analogue, Inhibitors of Mammalian Aromatase. Comparison with Natural Substrates: Prediction of Enantioselectivity for *N*-Alkyl Derivatives

Charles A. Laughton,† Robert McKenna,† Stephen Neidle,*,† Michael Jarman,‡ Ray McCague,‡ and Martin G. Rowlands‡

Cancer Research Campaign Biomolecular Structure Unit and Cancer Research Campaign Laboratories, Section of Drug Development, Institute of Cancer Research, Cotswold Road, Sutton, Surrey, SM2 5NG, U.K. *Received October 10, 1989*

Inhibitors of the cytochrome P450 enzyme aromatase, which is involved in the biosynthesis of estrogens from androgens, are of proven utility in the treatment of hormone-dependent breast cancer. The determination of the crystal structure of one such inhibitor, 3-ethyl-3-(4-pyridyl)piperidine-2,6-dione (2) and its 3-butyl analogue (3) is described. In the absence of three-dimensional structural information for the enzyme, conformational analysis and comparison with natural substrates has been performed in order to define possible "active" conformations. The enhanced inhibitory activity of 3 may be linked to hydrophobic interactions between the side chain and that portion of the enzyme that normally interacts with the B and C rings of a steroid substrate. Information gained from this study and previous studies by other workers has been combined in order to produce a hypothesis to explain the pattern of activity of *N*(1)-alkyl derivatives of 2. The successful application of this hypothesis to the prediction of the relative aromatase inhibitory activities of the two enantiomers of the *N*-octyl derivative (4) is described.

Aminoglutethimide (1; 3-(4-aminophenyl)-3-ethylpiperidine-2,6-dione) is currently in clinical use for the treatment of hormone-dependent breast cancer.[1] It inhibits the conversion of androgens into estrogens by means of direct interaction with the cytochrome P450 enzyme aromatase.[2] This reduces circulating estrogen levels, thereby reducing the stimulus required for the growth of hormone-dependent tumors. Aminoglutethimide has a chiral center at C(3) of the glutarimide ring. The *R* and *S* enantiomers have very different activities toward aromatase inhibition, the *R* isomer being 36 times more active.[3] This dependence on stereochemistry suggests that the chiral center and its environment is crucial for the binding of 1 to aromatase. Aminoglutethimide is also an inhibitor of another P450 enzyme, responsible for cholesterol side chain cleavage (desmolase).[4] This is responsible for the conversion of cholesterol into pregnenolone; its inhibition thus reduces the level of corticosteroid production. Patients treated with 1 must therefore receive hydrocortisone replacement therapy in order to counter this effect. Aminoglutethimide also has central nervous system (CNS) effects, producing drowsiness and ataxia.

The 4-pyridyl analogue (2; 3-ethyl-3-(4-pyridyl)-piperidine-2,6-dione) has been developed as a selective inhibitor of aromatase.[5] It does not inhibit desmolase, and in experimental studies does not produce the CNS side effects of 1;[6] it is now in clinical trial in the UK.

The present study reports on structural and conformational properties for 2[5] and its 3-butyl analogue 3,[7] (Figure 1) which has enhanced affinity for aromatase, in order to define possible "active" conformations in relation to the natural substrates. There is no structural information available at present on any of the eukaryotic P450 enzymes, so approaches to the rational design of substrate analogues must follow this more indirect approach. The successful application of these techniques to the prediction of the relative aromatase-inhibitory activities of the separate enantiomers of the *N*(1)-octyl derivative (4) of 2 is described.

* Address correspondence to this author.
† Biomolecular Structure Unit.
‡ Section of Drug Development.

Table I. Crystal Data

	2	3
formula	$C_{12}H_{14}N_2O_2$	$C_{14}H_{18}N_2O_2$
M_r	218	246
cell dimensions	a = 11.620 (2) Å b = 12.803 (3) Å c = 14.751 (6) Å	a = 12.239 (3) Å b = 24.888 (5) Å c = 8.990 (2) Å β = 105.22 (3)°
space group	$Pca2_1$	$P2_1/c$
Z	8	8
molecules/asymmetric unit	2	2
crystal size	0.2 × 0.2 × 0.01 mm	0.3 × 0.2 × 0.08 mm
data collection range	$1.5 < \theta < 65.0°$	$1.5 < \theta < 65.0°$
no. of unique reflns measured	1950	4647
no. of significant reflections	$1196 > 1.5\sigma(I)$	$2886 > 2.5\sigma(I)$
R	0.042	0.096
R_w	0.041	0.105

Results and Discussion

Crystal Structures. Both 2 and 3 crystallize with two independent molecules in the crystallographic asymmetric unit. This analysis is of their racemates; the coordinates and the computer plots of the molecular structure are of the R enantiomers (Figures 2 and 3), the *R* form having been shown, for 2 (though not yet for 3) to be 20-fold more inhibitory than the S form.[8]

(1) Lonning, P. E.; Kvinnsland, S. *Drugs* **1988**, *35*, 684.
(2) Chakraborty, J.; Hopkins, R.; Parke, D. V. *Biochem. J.* **1972**, *130*, 19.
(3) Graves, P. E.; Salhanick, H. A. *Endocrinology* **1979**, *105*, 52.
(4) Camacho, A. M.; Cash, R.; Brough, A. J.; Wilroy, R. J. *J. Am. Med. Assoc.* **1967**, *202*, 20.
(5) Foster, A. B.; Jarman, M.; Leung, C.-S.; Rowlands, M. G.; Taylor, G. N.; Plevey, R. G.; Sampson, P. J. *J. Med. Chem.* **1985**, *28*, 200.
(6) Foster, A. B.; Jarman, M.; Taylor, G. N.; Leung, C.-S. U.K. Patent 2151226A, 1985.
(7) Leung, C. S.; Rowlands, M. G.; Jarman, M.; Foster, A. B.; Griggs, L. J.; Wilman, D. E. V. *J. Med .Chem.* **1987**, *30*, 1550.
(8) McCague, R.; Jarman, M.; Rowlands, M. G.; Mann, J.; Thickitt, C. P.; Clissold, D. W.; Neidle, S.; Webster, G. *J. Chem. Soc., Perkin Trans. 1* **1989**, 196.

0022-2623/90/1833-2673$02.50/0

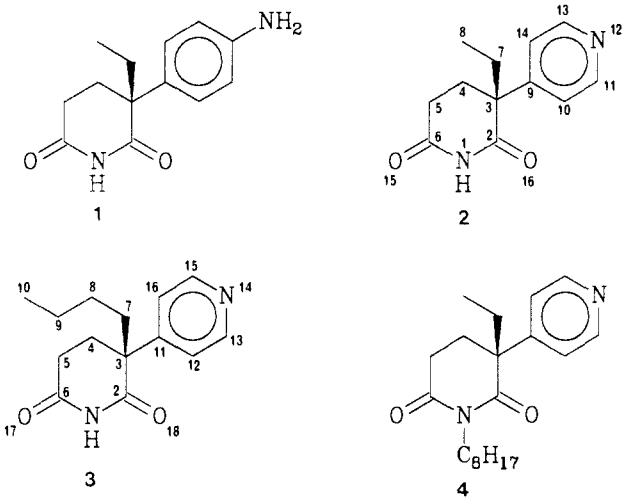

Figure 1. Structures and numbering for **1**, **2**, **3**, and **4**. For **2**, α = 2-3-7-8 and β = 2-3-9-10. For **3**, α = 2-3-7-8 and β = 2-3-11-12.

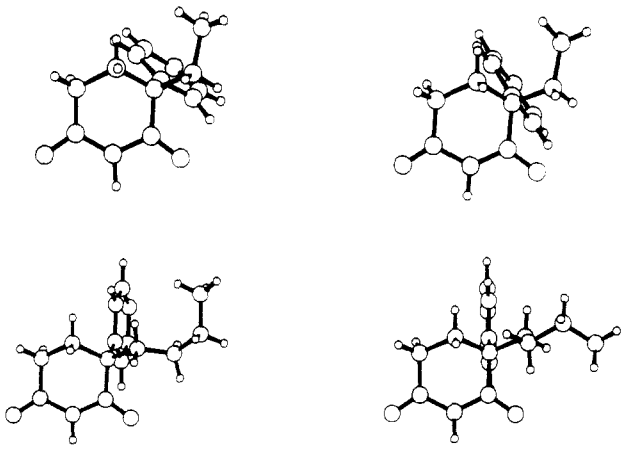

Figure 2. Plot of the X-ray structure conformation of (top) **2** and (bottom) the 3-butyl analogue **3**. Molecule a is shown in both cases on the left-hand side.

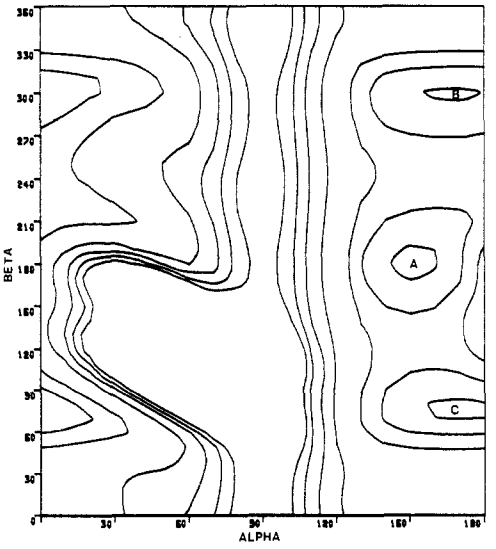

Figure 3. Contour plot of energy (kcal/mol) of **2** as a function of rigid rotations of α and β when ethyl group is pseudo-equatorial. Contours at 12, 15, 20, 40, 60, 80, and 100 kcal/mol. Local minima A–C marked.

The two molecules have very similar, though nonidentical, conformations (Table IV). Thus, although the glu-

Table II. Positional Parameters and Their Estimated Standard Deviations[a]

atom	x	y	z	B (Å^2)
		(a) For **2**		
N1A	0.8810 (4)	0.5424 (3)	0.721	3.00 (9)
C4A	1.0854 (5)	0.5557 (4)	0.6134 (4)	3.1 (1)
C6A	0.9297 (5)	0.6413 (4)	0.7058 (4)	3.5 (1)
C13B	0.1106 (5)	0.9784 (4)	0.6248 (3)	3.3 (1)
C4B	-0.704 (4)	0.9628 (4)	0.8777 (3)	2.8 (1)
C14B	0.0432 (4)	0.9810 (4)	0.7013 (3)	2.6 (1)
N12B	0.1938 (4)	0.0478 (3)	0.6061 (3)	3.3 (1)
C6B	0.1096 (5)	0.9055 (4)	0.9612 (4)	3.2 (1)
C2A	0.9144 (5)	0.4533 (4)	0.6653 (4)	3.0 (1)
C3B	-0.0098 (4)	1.0658 (4)	0.8531 (3)	2.3 (1)
C10B	0.1490 (4)	1.1285 (4)	0.7482 (4)	2.6 (1)
N12A	0.8162 (4)	0.4997 (4)	0.3370 (3)	3.6 (1)
O2B	0.0890 (3)	1.1819 (3)	0.9573 (3)	3.83 (8)
C9B	0.0621 (4)	1.0572 (4)	0.7664 (4)	2.3 (1)
C3A	1.0052 (4)	0.4649 (3)	0.5908 (3)	2.4 (1)
C5A	1.0231 (5)	0.6557 (4)	0.6413 (4)	3.5 (1)
N1B	0.1290 (4)	1.0126 (3)	0.9723 (3)	2.91 (9)
C14A	0.9584 (4)	0.5613 (4)	0.4421 (4)	2.6 (1)
C11B	0.2110 (5)	1.1219 (4)	0.6691 (4)	3.1 (1)
C2B	0.0712 (4)	1.0925 (4)	0.9315 (3)	2.4 (1)
O6A	0.8890 (4)	0.7110 (3)	0.7532 (3)	5.3 (1)
C7B	-0.982 (5)	1.554 (4)	0.8426 (4)	3.4 (1)
C7A	1.0751 (5)	0.3602 (4)	0.5884 (4)	3.2 (1)
C11A	0.8024 (5)	0.4174 (4)	0.3929 (4)	3.7 (1)
C13A	0.8948 (5)	0.5692 (4)	0.3633 (4)	3.7 (1)
C9A	0.9409 (4)	0.4785 (3)	0.5011 (3)	2.3 (1)
C5B	0.0144 (5)	0.8759 (4)	0.9002 (4)	3.4 (1)
O2A	0.8684 (3)	0.3717 (3)	0.6841 (3)	4.8 (1)
O6B	0.1721 (4)	0.8452 (3)	0.9993 (3)	5.2 (1)
C10A	0.8612 (4)	0.4038 (4)	0.4735 (4)	3.0 (1)
C8B	-0.1841 (5)	1.1395 (4)	0.7669 (4)	3.9 (1)
C8A	1.1643 (5)	0.3549 (4)	0.5136 (4)	4.1 (1)
		(b) For **3**		
N1A	0.3383 (5)	0.4826 (3)	0.4985 (8)	2.3 (2)
C6B	0.9321 (8)	0.1718 (4)	0.400 (1)	3.2 (2)
C2B	0.7824 (7)	0.2230 (4)	0.481 (1)	2.5 (2)
C16B	0.6185 (6)	0.0972 (4)	0.538 (1)	2.3 (2)
C11B	0.6877 (6)	0.1427 (4)	0.5659 (9)	1.9 (2)
N14B	0.6615 (6)	0.0784 (3)	0.8072 (9)	2.9 (2)
O2A	0.1876 (6)	0.5136 (3)	0.3213 (9)	4.1 (2)
C6A	0.4198 (7)	0.4452 (4)	0.566 (1)	2.7 (2)
C12B	0.7427 (8)	0.1550 (4)	0.716 (1)	2.6 (2)
O2B	0.7596 (6)	0.2632 (3)	0.5376 (9)	4.2 (2)
C5A	0.4222 (7)	0.3942 (4)	0.479 (1)	2.9 (2)
C3A	0.2442 (7)	0.4241 (4)	0.279 (1)	2.2 (2)
C15B	0.6080 (7)	0.0665 (4)	0.660 (1)	2.7 (2)
C2A	0.2529 (7)	0.4770 (4)	0.364 (1)	2.2 (2)
C15A	0.0504 (8)	0.3594 (5)	0.504 (1)	3.9 (2)
O6B	1.0269 (5)	0.1727 (3)	0.3857 (9)	4.4 (2)
C7A	0.1878 (8)	0.4308 (4)	0.104 (1)	3.1 (2)
C13B	0.7287 (8)	0.1220 (5)	0.834 (1)	3.4 (2)
C16A	0.1146 (7)	0.3987 (4)	0.453 (1)	3.3 (2)
C4A	0.3646 (7)	0.4003 (4)	0.307 (1)	2.8 (2)
C12A	0.1513 (7)	0.3329 (4)	0.286 (1)	3.0 (2)
N14A	0.0340 (6)	0.3107 (3)	0.451 (1)	3.7 (2)
C3B	0.6966 (7)	0.1771 (4)	0.428 (1)	2.3 (2)
C8A	0.2581 (9)	0.4618 (5)	0.015 (1)	4.9 (3)
N1B	0.8874 (6)	0.2168 (3)	0.4570 (9)	2.5 (2)
C5B	0.8548 (8)	0.1246 (4)	0.362 (1)	3.7 (2)
C4B	0.7337 (8)	0.1404 (4)	0.306 (1)	3.6 (2)
C13A	0.0847 (8)	0.2984 (4)	0.343 (1)	3.9 (2)
C11A	0.1693 (6)	0.3847 (4)	0.342 (1)	2.2 (2)
C9A	0.199 (1)	0.4614 (5)	-0.159 (1)	5.0 (3)
O6A	0.4860 (6)	0.4549 (3)	0.6890 (8)	4.7 (2)
C7B	0.5782 (8)	0.2003 (5)	0.344 (1)	4.2 (3)
C8B	0.513 (1)	0.2285 (5)	0.438 (2)	5.7 (3)
C9B	0.388 (1)	0.2380 (6)	0.352 (2)	6.8 (4)
C10A	0.105 (1)	0.4976 (6)	-0.197 (2)	7.0 (4)
C10B	0.315 (1)	0.1880 (9)	0.320 (3)	13.9 (7)

[a] Anisotropically refined atoms are given in the form of the isotropic equivalent thermal parameter defined as $(^4/_3)[a^2B(1,1) + b^2B(2,2) + c^2B(3,3) + ab(\cos\gamma)B(1,2) + ac(\cos\beta)B(1,3) + bc(\cos\alpha)B(2,3)]$.

Table III. Parameterization of **2** for MMP2(85)

type	parameter[a]	values	source
bending	3-9-3	B = 0.76 T = 127.0	force constant from 1-9-3, angle from crystal structure
torsion	2-1-3-9	V1 = 0.0, V2 = 0.0, V3 = 0.4	1-1-3-9
torsion	1-3-8-3	V1 = 0.0, V2 = 5.0, V3 = 0.0	1-3-9-1
torsion	7-3-9-3	V1 = 0.0, V2 = 5.0, V3 = 0.0	1-3-9-1

[a] Numbers refer to MM2 atom types.

Table IV. Derived Structural Data, Calculated from the Crystallographic Coordinates[a]

(a) **2**

	least-squares plane of the glutarimide ring: deviations of atoms from plane, Å	
	molecule A	molecule B
C6	−0.023 (6)	−0.052 (6)
O6	−0.005 (4)	−0.012 (4)
N1	0.036 (3)	0.036 (4)
C2	0.018 (5)	0.048 (5)
O2	−0.027 (4)	−0.044 (4)
*H1	0.087 (52)	0.003 (50)
*C3	0.098 (5)	0.226 (5)
*C4	−0.530 (5)	−0.571 (5)
*C5	−0.059 (6)	−0.174 (6)

		molecule A	molecule B
angle between glutarimide plane, defined above, and pyridine ring, deg		104.6 (5)	95.7 (5)
torsion angles, deg	N1-C2-C3-C4	29.6 (5)	38.6 (5)
	C2-C3-C7-C8 (β)	176.0 (6)	179.9 (6)
	C2-C3-C9-C14 (α)	125.5 (6)	139.7 (6)

(b) **3**

	least-squares plane deviations, Å	
	molecule A	molecule B
C6	−0.013 (9)	0.016 (10)
O6	0.019 (7)	0.002 (8)
N1	−0.026 (7)	−0.022 (7)
C2	0.015 (9)	−0.014 (9)
O2	0.004 (7)	0.018 (7)
*H1	−0.056 (24)	−0.053 (23)
*C3	0.105 (9)	−0.086 (9)
*C4	−0.627 (9)	−0.646 (9)
*C5	−0.057 (9)	0.080 (10)

		molecule A	molecule B
angle between glutarimide and pyridine rings, deg		91.5 (13)	102.7 (13)
torsion angles, deg	N1-C2-C3-C4	31.1 (13)	19.3 (14)
	C2-C3-C7-C8 (β)	−68.5 (14)	71.4 (14)
	C2-C3-C11-C14 (α)	178.1 (14)	175.0 (14)
	C3-C7-C8-C9	5.2 (15)	166.3 (16)
	C7-C8-C9-C10	−75.7 (16)	−69.4 (17)

[a] Atoms marked (*) have been excluded from the calculation of the plane itself.

tarimide rings have a half-chair conformation with ring atom C(4) deviating from the least-squares plane in both cases, molecule **2b** has greater ring pucker as a whole. The torsion angle α defines the orientation of the pyridine ring—it differs by 14° in the two molecules. The ethyl group is orientated trans to the glutarimide ring in both molecules. They adopt an overall V shape.

The two independent molecules of **3** retain the same type of glutarimide ring pucker and this overall molecule shape, although the orientations of the butyl side chain, as defined by angle β, now differ by 140°.

Conformational Analysis of 2. Minimization of molecule **2b** (to local minimum A) resulted in only very small movements in the non-hydrogen atoms (a rms shift of 0.17 Å for all atoms and 0.09 Å for the non-hydrogen ones). There was a slight increase in the degree of glutarimide ring pucker and a reduction in the angle α from −41.9° to −35.0°. Minimization of molecule **2a** produced greater overall movements, with a rms shift of 0.37 Å for all atoms and 0.26 Å for the non-hydrogens. This minimization corresponded to relaxation to the same local minimum A, but from further away.

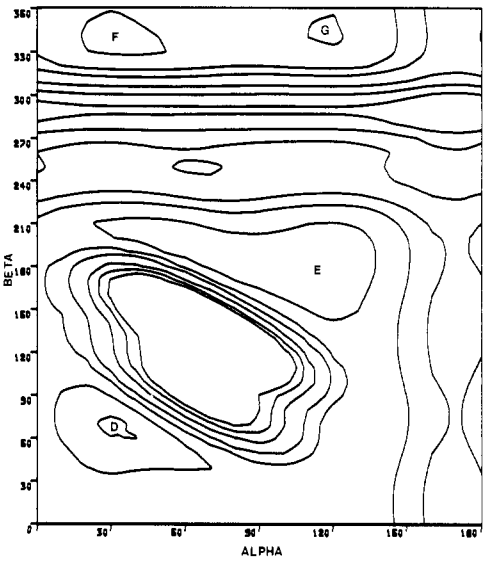

Figure 4. Contour plot of energy (kcal/mol) **2** as a function of rigid rotations of α and β when ethyl group is pseudo-axial. Contours at 15, 20, 30, 40, 60, 80, and 100 kcal/mol. Local minima D–G marked.

A conformational search over the angles α and β (in 10° intervals) was performed with use of the minimized conformation A (local minimum A). This led to the identification of two further local minima B and C (Figure 3), corresponding to a first approximation to the two other possible staggered conformations of the ethyl group. The exact location of each was found by full minimization starting from suitable values of α and β (see Table V).

MM2 calculations also revealed an alternative minimum energy conformation for the glutarimide ring, corresponding to the pyridyl group adopting a pseudoequatorial position rather than the pseudoaxial position found in the crystal structure conformations. A conformational search over α and β revealed four local minima, D–G (Figure 4), in general less sharply defined than those for the alternative glutarimide ring conformation and all of higher energy than A–C (Table V).

Modeling 2 and Androstenedione. A study of the structural relationships between a number of aromatase inhibitors and the natural substrate androstenedione has been published previously.[12] Aminoglutethimide was included in this study but not **2**. We have applied the methodology used in this analysis to the latter drug. The working model for the active site of aromatase was developed from an analysis of both steroid-like and non-steroid-like inhibitors and substrates. This led to the prediction of two hydrogen bond donor groupings in the active site which might interact with the C(3) and C(17) functions of the natural substrates plus a hydrophobic cleft to interact with the steroid backbone. The activity of structurally diverse inhibitors led to the postulation of two further potential binding sites, a hydrophobic pocket extending out from the region occupied by C(4) of a steroid substrate, and the heme group which should lie above the

Table V. Structures and Energies of Conformations of **2**

conformation	energy, kcal/mol	torsion angles, deg					
		α	β	1-2-3-4	2-3-4-5	3-4-5-6	4-5-6-1
crystal a	168.0	125	176	30	-48	45	-16
crystal b	109.0	139	180	39	-55	46	-21
A	11.0	152	180	38	-62	56	-22
B	10.5	173	76	38	-62	56	-23
C	10.7	171	-62	36	-61	57	-25
D	15.2	33	68	-28	54	-54	27
E	13.1	116	180	-35	58	-53	22
F	14.7	33	-32	-25	51	-52	27
G	16.6	116	-13	-32	58	-56	26

Table VI. Superimposition of Conformers of **2** over Androstenedione

conformation	distances (Å) of selected steroid atoms from pyridyl nitrogen atom		
	C(3)	C(17)O	C(19)
A	6.4	9.2	3.2
B	6.5	9.3	3.2
C	6.2	9.2	3.3
D	8.2	6.0	3.5
E	8.4	5.1	3.8
F	8.1	6.4	3.4
G	8.3	5.5	3.7
aminoglutethimide[a]	9.2	7.6	4.5

[a] From ref 9.

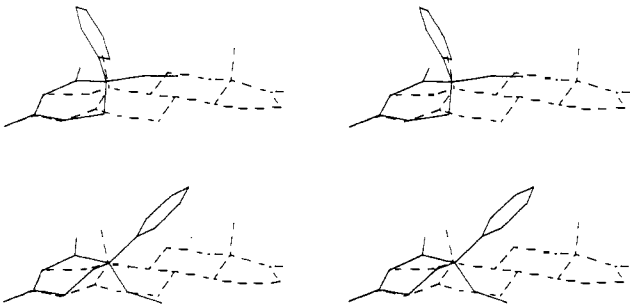

Figure 5. Stereoplots of conformers A (top) and E (bottom) of **2** superimposed over androstenedione.

position occupied by C(19) of such substrates.

For each local minimum conformation a superimposition over androstenedione was performed by means of a least-squares fit of atoms O(20), C(2) and N(1) of **2** to atoms C(3)O, C(3) and C(2) of the steroid, respectively. This places the pyridyl nitrogen atom in an area above the β-face of the steroid, close to the C(19) methyl group where it may coordinate to the enzyme heme group and the ethyl group in an area where it may mimic a portion of the B and C rings (Figure 5). A better overall fit can be obtained if further atom pairs are included for the superimposition; however, the protocol above allows direct comparison with results previously reported.[9]

The results of this study are presented in Table VI. Comparison with Table III in ref 9 reveals that for all conformers the position of the putative coordinating nitrogen atom above the steroid ring lies outside the range of positions generally observed for other inhibitors. The situation can be improved somewhat by relaxing the exactitude of the fitting procedure, but only to an appreciable extent for the conformers D–G, in which the pyridyl group is in the (considerably less favored) equatorial position. In view of the energy difference between conformations A–C and D–G that results from the adoption of the alternative glutarimide ring pucker, the noninclusion in the previous study of conformers of **1** in which the aniline group adopted the axial position would appear unwarranted.

Conformational Analysis of the Butyl Analogue 3. Minimization of molecule **3a** (to local minimum A) led to marked movements in both the butyl chain and glutarimide ring (Table VII). Rms shifts were 0.387 Å for all atoms and 0.278 Å for non-hydrogen atoms. In contrast minimization of molecule **3b** (to local minimum B) resulted in much smaller movements (rms shifts of 0.224 Å for all atoms, 0.139 Å for non-hydrogen atoms). The two minima differ, to a first approximation, only in their value of β (77° for minimum A, -63° for B).

In view of the extra degrees of freedom associated with the butyl chain no detailed conformational analysis was attempted. In both crystal structure conformations (and their derived local minima) the butyl chain is not all-trans. The fully extended conformation derived from local minimum A was minimized (to local minimum C), the difference in energy between the two proved small (see Table VII). Finally, for modeling purposes, conformation C was manipulated to set β to 180 deg and again minimized (to local minimum D).

Modeling Studies on the Butyl Analogue 3. The small energy difference between the local minima found for **3** suggests that, dynamically, the butyl chain sweeps out a large volume of space, hindering any static modeling-based analysis. However, it is clear that superimposition of the molecule over androstenedione as described for **2** leads to the butyl group projecting in the general direction of the B, C, and D rings, and that a very good overlap is possible; see Figure 6 for local minimum D. The observation that the inhibitory activity of analogues of **2** in which the ethyl group is replaced with a longer alkyl group increases with chain length up to a maximum at *n*-octyl (see Table VIII) may thus be explained in terms of an improving mimicry of the hydrophobic region of the natural substrates.

The Activity of N(1)-Substituted Derivatives. It has been observed that the alkylation of **2** at N(1) leads to derivatives whose aromatase inhibitory activity shows an interesting dependence on chain length. As chain length increases there is an initial sharp decrease in activity to ethyl followed by a slow increase, the activity of the unsubstituted compound only being exceeded above pentyl and reaching a maximum at octyl (see Table VIII).[7] Although comparable data with androstenedione as substrate has not been obtained (only **2** and its *N*-octyl analogue having been evaluated) it is a plausible assumption that the ranking of analogues would be comparable with this substrate.

(9) Banting, L.; Smith, H. J.; James, M.; Jones, G.; Nazareth, W.; Nichols, P. J.; Hewlins, M. J. E.; Rowlands, M. G. *J. Enzyme Inhib.* **1988**, *2*, 215.

Table VII. Structures and Energies of Conformations of 3

conformation	energy, kcal/mol	torsion angles, deg			
		α	β	3-7-8-9	7-8-9-10
crystal a	181.3	178	-69	-175	-69
crystal b	183.4	175	71	166	-76
A	12.4	172	77	-175	-66
B	12.8	170	-63	177	-69
C	11.6	172	78	-176	-178
D	12.1	148	180	179	-180

Table VIII. Inhibition of Aromatase by Alkyl Analogues of 2

	alkyl derivatives	IC_{50},[a] μM
C(3)	methyl	245
	ethyl	10
	propyl	6
	butyl	4
	pentyl	2.5
	hexyl	3.6
	heptyl	3.2
	octyl	0.33
	nonyl	2.4
N(1)	methyl	30
	ethyl	385
	propyl	31
	butyl	40
	pentyl	21
	hexyl	6.6
	heptyl	1.5
	octyl	0.8
	nonyl	3.0
	decyl	10

[a] Concentration giving 50% inhibition of enzyme activity.[7]

Such a pattern of behavior would be difficult to rationalize on the basis of the model so far developed; the superimposition of 1 and androstenedione places the glutarimide nitrogen in the region of C(2) of the steroid, and there is evidence that the introduction of steric bulk in this region is not favorable for aromatase inhibition.[10] However, we can postulate an alternative mode of superimposition, in which the C(6) carbonyl group of the glutarimide ring still mimics the C(3) carbonyl group of the steroid but now the glutarimide nitrogen atom occupies the area corresponding to C(4) of the steroid, where there is evidence for the existence of a hydrophobic pocket.[10-12]

However, in this binding mode the pyridyl group no longer projects in the direction of the heme group unless we model the *S* enantiomer (Figure 7), which is known to be of considerably lower activity in the case of 2. Yet the fitting of the *S* isomer in this alternative mode appears at least as good as that of the *R* enantiomer in the originally developed mode, so other factors, possibly electrostatic in origin, may account for this difference in activity.

Putting these observations together we arrive at a possible explanation for the observed behavior of the *N*-alkyl analogues of 2. Introduction of a *N*-alkyl group inhibits binding of the *R* isomer in the original mode where the nitrogen atom mimics C(2) of a steroid; however, the alternative mode of binding available to the *S* isomer is not favored until the alkyl chain is large enough for the extra hydrophobic interaction available in this mode to outweigh the inherent unfavorable electrostatic term.

Obviously to test the validity of the foregoing hypothesis we require the biological testing of the separate enantiomers of the *N*-alkyl derivatives. We have therefore synthesized and tested the individual enantiomers of the most active *N*-alkyl derivative, namely the *N*-octyl derivative (4). These were prepared from the separate enantiomers of 2 by alkylation with bromooctane in the presence of cesium carbonate as base.[7] As with 2 the *R* enantiomer was dextrorotatory. The dose-response curves are shown in Figure 8. In evaluating the results it should be noted that the aromatization of androstenedione (chosen as substrate for consistency with the modeling studies) is much less efficiently inhibited by the racemic (4) than is aromatization of testosterone. The respective IC_{50} values are 5 and 0.8 μm in a previous test.[7] The present enzyme preparation gave a somewhat lower IC_{50} value (20 μm) than previously reported for the racemate. However, the results clearly support the prediction of the model, in that only the *S* enantiomer is inhibitory, having an IC_{50} value (9 μM) almost one-half that of the racemate, as would be expected. Under similar conditions, aminoglutethimide gives an IC_{50} value of 30 μM.

As further evidence, the placental cytochrome P450 difference binding spectra were determined for each enantiomer of 4. The *S* enantiomer displayed a Type II binding spectra characterized by an absorbance maximum at 425 nm and a minimum between 390 and 410 nm. The apparent spectral dissociation constant K_s was 0.51 μM. On the other hand, the *R* enantiomer gave no difference binding spectra, even when added to a final concentration

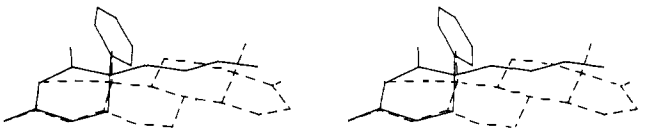

Figure 6. Stereoplot of conformer D of 3 superimposed over androstenedione.

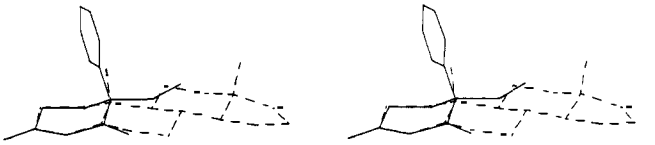

Figure 7. Stereoplot of *S*-2 (mirror image of conformer A) superimposed over androstenedione.

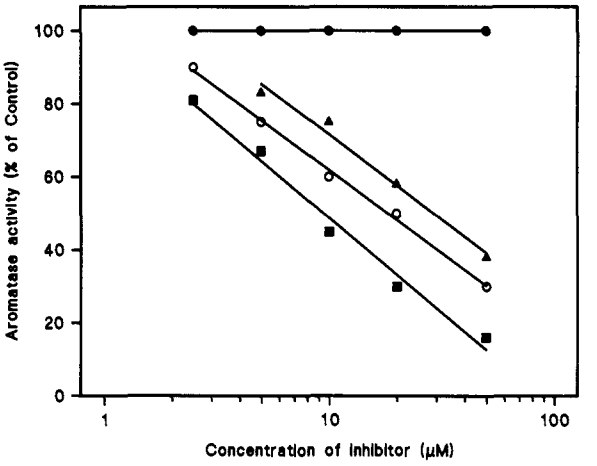

Figure 8. Inhibition of the aromatization of androstenedione by the racemic *N*-octyl derivative (4) (○), its *S* enantiomer (■), and its *R* enantiomer (●). Aminoglutethimide (1) is shown for comparison (▲). Each point is the mean of triplicate determinations (±10%).

(10) Brueggemeier, R. W.; Floyd, E. E.; Counsell, R. E. *J. Med. Chem.* **1978**, *21*, 1007.
(11) Darby, M. V.; Lovett, J. A.; Brueggemeier, R. W.; Groziak, M. P.; Counsell, R. E. *J. Med. Chem.* **1985**, *28*, 803.
(12) Abul-Hajj, Y. J. *J. Med. Chem.* **1986**, *29*, 582.

of 100 μM. Both 1 and 2 display a Type II binding spectra in their interaction with placental cytochrome P450.[3,5] This type of binding spectrum is due to the coordination of the 4-pyridyl or aniline group with the iron atom in the heme of cytochrome P450.

In summary, the results presented here, in particular the successful prediction of the relative activities of the enantiomers of the *N*-octyl derivative 4, support in general terms the model for the relationship between the steroid skeleton and structurally diverse aromatase inhibitors that has been previously described.[9] In relation to that study two particular points emerge. Firstly that the distance between the atoms mimicing a portion of the mean steroid plane and that interacting with the heme is not critical, e.g. comparing 1 and 2. Secondly that the question of the conformation adopted by substituted glutarimide rings should be considered carefully; the rejection of the axial conformation of aminoglutethimide many not have been valid.

An important question this study illustrates, but cannot explain, concerns the underlying cause of the difference in activity between the *R* and *S* enantiomers of glutarimide derivatives; this question probably cannot be answered until some information is available as to the three-dimensional structure of the active site of aromatase.

In relation to certain aromatase inhibitors,[13] such as CGS 16949A,[14] LY 113174,[15] and R 76713,[16] compound 2 is not a very potent aromatase inhibitor; however, the modeling shows that there is much scope for improvement, e.g. in developing parts of the molecule to mimic portions of the C and D rings of a steroid, and to exploit the hydrophobic pocket that extends from the position occupied by C-4 of steroid substrates. The validation of our model with the enantiomer studies means that such strategies for the design of new aromatase inhibitors may go ahead with some confidence.

Experimental Section

Crystallographic Studies. Colorless, plate-like crystals of 2 and 3, were grown from ethanol. Preliminary cell dimensions and information on crystal symmetry were obtained from Weissenberg and oscillation photographs. Accurate cell dimensions were obtained from least-squares refinements of 25 θ values for each crystal measured on an Enraf-Nonius CAD4 diffractometer. Intensity data were collected on the diffractometer with an $\omega - 2\theta$ scan technique and graphite-monochromated Cu Kα radiation. Three standard reflections were monitored every 3600 sec of beam time; no crystal decay was observed. Crystal and other relevant data are given in Table I.

The structures were solved by direct methods using the MULTAN82 program. In both cases, the phase set with the highest combined figure of merit revealed the correct structure. Refinement was by full-matrix least-squares methods, with anisotropic thermal parameters for the non-hydrogen atoms. Hydrogen atom positions were generated by standard geometric considerations; their parameters were not refined. An empirical absorption correction was applied to both data sets, together with a weighting scheme of the form

$$W = [\sigma^2(F) + (0.04|F|^2]^{-1}$$

Final electron density maps did not show any significant features greater than 0.4 e Å^{-3}. Fractional coordinates for the non-hydrogen atoms are given in Table II. Tables of hydrogen atom coordinates, anisotropic thermal parameters, and bond lengths and angles have been deposited as supplementary material.

Molecular Modeling. All molecular mechanics calculations were performed by using the program MMP2(85)[17] running on a VAX 11/751 computer. Graphical display and manipulation was performed by using the GEMINI program[18] running on an Iris 3130 workstation. The molecular structures of the two 2 and 3 were taken from the X-ray data. For calculations using MMP2(85) a lone pair was added to the pyridine nitrogen atom and extra parameters for the glutarimide ring were required; their values and source are given in Table III. The structure of androstenedione was obtained by minimization of the crystal structures of 6β-bromo-4-androstene-3,17-dione[19] after substitution of a hydrogen atom for the bromine. Minimizations were performed with the default conditions, except that dipole interaction energies were calculated for all interactions. For the two-dimensional conformational searches, the relevant angles were driven through the range in ten-degree intervals with the minimization step suppressed. In order to generate the conformations of 2 in which the ethyl group adopted the pseudo-axial position, torsion angle C(2)–C(3)–C(4)–C(5) was driven from −55° to +45° in ten-degree intervals followed by a full, free, energy minimization.

Enantiomers of 3-Ethyl-1-octyl-3-(4-pyridyl)piperidine-2,6-dione. Either *R*-(+)- or *S*-(−)-2[8] (22 mg, 0.1 mmol), Cs_2CO_3 (100 mg), and 1-bromooctane (39 mg, 0.2 mmol) in MeCN (1 mL) were heated under reflux with stirring until reaction was judged complete by TLC on silica gel (in CH_2Cl_2–EtOH, 19:1; UV detection with a Hanovia chromatolite). The products were isolated as colorless oils by successive preparative TLC (Merck Kieselgel 60, 20 × 20-cm glass plates, 2-mm layers) first in Et_2O, then (to remove colored impurities), in CH_2Cl_2–EtOH, 19:1. The products gave NMR spectra identical with racemic 3-ethyl-1-octyl-3-(4-pyridyl)piperidine-2,6-dione: ($CDCl_3$, 250 MHz recorded on a Bruker AC250 spectrometer) δ_H 0.87 (t, 6, J = 7.3 Hz, 2 × CH_3), 1.20–1.36 (m, 10), 1.42–1.58 (m, 2), 1.89 (m, 1, CH_2 of Et), 2.07 (m, 1, CH_2 of Et), 2.16–2.48 (m, 3, glutarimide ring), 2.68 (m, 1, glutarimide ring), 3.80 (apparent dd, 2, J = 6.5, 8.5 Hz, NCH_2), 7.15 (m, 2, pyridyl), 8.58 (m, 2, pyridyl). *S* enantiomer: $[\alpha]^{20}_D$ = −119° (c = 0.35 in MeOH). Anal. ($C_{20}H_{30}N_2O_2$), C, H, N. *R* enantiomer: $[\alpha]^{20}_D$ = +117° (c = 0.35 in MeOH). Anal. H, N; C: calcd 72.7; found 72.0.

Aromatase Assays and Binding Spectra of Enantiomers of 3-Ethyl-1-octyl-3-(4-pyridyl)piperidine-2,6-dione (4). Aromatase was obtained from the microsomal fraction of full-term human placentas. The activity was monitored by measuring the ^3H_2O formed during the conversion of [1-^{3}H]androstenedione into estrone. The K_m value for androstenedione was 0.0375 μm so a final substrate concentration of 0.375 μm was used. The dose-response curves shown in Figure 8 were calculated by linear regression. The IC_{50} value is the concentration of compound required to reduce the activity of the enzyme to 50% of its control value at the stated substrate concentration. Assay concentrations of 0, 2.5, 5.0, 10.0, 20.0, and 50.0 μM were used. Difference binding spectra were obtained at room temperature with a Pye Unicam SP8-150 spectrophotometer in the range 360–480 nm. The human placental microsomes were diluted with 0.05 M potassium phosphate buffer (pH 7.4) to give a final protein concentration of 4 mg/mL. The ligands were dissolved in dimethyl sulfoxide and equal volumes of solvent were added to the reference and

(13) Van Wauwe, J. P.; Janssen, P. A. *J. Med. Chem.* **1989**, *32*, 2231.
(14) Steele, R. E.; Mellor, L.; Sawyer, W. K.; Wasvary, J. M.; Browne, L. J. *Steroids* **1987**, *50*, 147.
(15) Hirsch, K. S.; Jones, C. D.; Lindstrom, T. D.; Stamm, N. B.; Sutton, G. P.; Taylor, H. M.; Weaver, D. E. *Steroids* **1987**, *50*, 201.
(16) Wouters, W.; DeCoster, R.; Krekels, M.; van Dun, J.; Beerens, D.; Haelterman, C.; Raeymaekers, A.; Freyne, E.; Van Gelder, J.; Venet, M.; Janssen, P. A. J. *J. Steroid Biochem.* **1989**, *32*, 781.
(17) N. L. Allinger; Y. Yuh, available from QCPE, Dept. of Chemistry, Indiana University, Bloomington, IN 47405.
(18) The molecular modeling program GEMINI, written by Dr. A. Beveridge, at the Institute of Cancer Research, is available from Hampden Data Services Ltd., Foxcombe Court, Wyndyke Business Park, Abingdon, Oxon, OX14 1DZ.
(19) Strong, P. D.; Hazel, J. P.; Duax, W. L.; Osawa, Y. *Cryst. Struct. Commun.* **1976**, *275*, 5.

sample curvettes. Dimethyl sulfoxide had no effect on the binding spectra with addition up to 10% of the final suspension volume. The K_s value was determined from a Scatchard plot (absorbance difference vs absorbance difference/concentration = slope K_s) and is the average of three determinations (±10%).

Acknowledgment. This work was supported by grants from the Cancer Research Campaign (to the Biomolecular Structure Unit) and from the Cancer Research Campaign/Medical Research Council (to the Section of Drug Development).

Supplementary Material Available: Tables listing hydrogen atom coordinates, anisotropic thermal parameters, and bond lengths and angles (19 pages). Ordering information is given on any current masthead page.

Additions and Corrections

1990, Volume 33

Mark G. Bock,* Robert M. DiPardo, Ben E. Evans, Kenneth E. Rittle, Willie L. Whitter, Daniel F. Veber, Roger M. Freidinger, Raymond S. L. Chang, T. B. Chen, and Victor J. Lotti: Cholecystokinin-A Receptor Ligands Based on the κ-Opioid Agonist Tifluadom.

Page 451. The structure for **2** is incorrect. The correct structure is

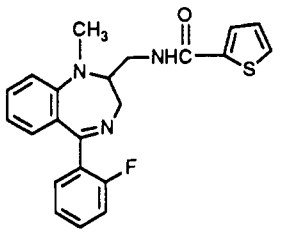

2, (*R*, *S*)-tifluadom
2a, (*R*)-(+)-tifluadom
2b, (*S*)-(−)-tifluadom

Robin D. Clark,* Jacob Berger, Pushkal Garg, Klaus K. Weinhardt, Michael Spedding,* Andrew T. Kilpatrick, Christine M. Brown, and Alison C. MacKinnon: Affinity of 2-(Tetrahydroisoquinolin-2-ylmethyl)- and 2-(Isoindolin-2-ylmethyl)imidazolines for α-Adrenoceptors. Differential Affinity of Imidazolines for the [^{3}H]Idazoxan-Labeled α_2-Adrenoceptor vs the [^{3}H]Yohimbine-Labeled Site[1].

Page 597. Structure **6a,b** in Table I is incorrect. The correct structure is on page 596.

Page 597. The last sentence of the Chemistry section should read "Isoindolines **8a,b** ..." rather than **10a,b**.

C. David Jones,* Mark A. Winter, Kenneth S. Hirsch, Nancy Stamm, Harold M. Taylor, Howard E. Holden, James D. Davenport, Eriks V. Krumkalns, and Robert G. Suhr: Estrogen Synthetase Inhibitors. 2. Comparison of the in Vitro Aromatase Inhibitory Activity for a Variety of Nitrogen Heterocycles Substituted with Diarylmethane or Diarylmethanol Groups.

Page 419, Table IV, route 1. The structures for **70** and **43** are incorrect. The correct structures are

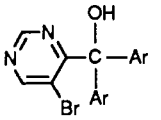

70

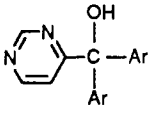

43

Gloria Cristalli, Palmarisa Franchetti, Mario Grifantini,* Giuseppe Nocentini, and Sauro Vittori: 3,7-Dideazapurine Nucleosides. Synthesis and Antitumor Activity of 1-Deazatubercidin and 2-Chloro-2′-deoxy-3,7-dideazaadenosine.

Page 1466. The ^{1}H NMR data for compound **18** (2′-deoxy-β-D-ribofuranosyl derivative) should read: δ 6.09 (s, 2, NH_2), 6.22 (pt, 1, C_1-H), 6.68 (d, 1, J = 3 Hz, C_3-H), 6.79 (d, 1, J = 6 Hz, C_7-H), 7.38 (d, 1, J = 3 Hz, C_2-H, 7.56 (d, 1, J = 6 Hz, C_6-H).